Schlecht, Sebastian J.; Sinjanakhom, Tantep; Välimäki, Vesa

Multi-shelf graphic equalizer

Published in:
Signal Processing

DOI:
10.1016/j.sigpro.2024.109630

Published: 01/01/2025

Document Version
Publisher's PDF, also known as Version of record

Please cite the original version:
Schlecht, S. J., Sinjanakhom, T., & Välimäki, V. (2025). Multi-shelf graphic equalizer. *Signal Processing*, *226*, Article 109630. https://doi.org/10.1016/j.sigpro.2024.109630

Signal Processing 226 (2025) 109630

Contents lists available at ScienceDirect

Signal Processing

journal homepage: www.elsevier.com/locate/sigpro

Multi-shelf graphic equalizer

Sebastian J. Schlecht [a,b], Tantep Sinjanakhom [a], Vesa Välimäki [a,*]

[a] Acoustics Lab, Department of Information and Communications Engineering, Aalto University, Espoo, 02150, Finland
[b] Multimedia Communications and Signal Processing, Friedrich-Alexander-Universität Erlangen-Nürnberg, Erlangen, 91054, Germany

ARTICLE INFO

Dataset link: https://github.com/SebastianJiroSchlecht/MultiShelfGEQ

Keywords:
Audio systems
Digital filters
Filtering algorithms
IIR filters
Optimization

ABSTRACT

A graphic equalizer (GEQ) is a standard tool in audio production and effect design. Adjustable gain control frequencies are fixed along the logarithmic frequency axis, and an automatic design method matches the magnitude response to them whenever target gains are changed. Most commonly, the GEQ comprises a set of peak filters centered an octave apart, possibly with a shelving filter at the bottom and top of the frequency range. While accurate designs were proposed, the dynamic range is typically limited to 24 dB. In this paper, we propose two innovations. First, we introduce a GEQ based on shelving filters only, which can cover an extensive dynamic range of over 60 dB. Secondly, we introduce an order-switching technique that combines shelf filters of different order. We demonstrate the performance and advantages of the proposed filter with design examples. The proposed shelf-filter-based GEQ offers a wider dynamic range and a smoother magnitude response than traditional peak-filter-based GEQ designs.

1. Introduction

Graphic equalizers (GEQ) have a long history in audio technology [1,3]. The first GEQs, which were based on analog electronics, were developed for cinemas in the 1950s to improve the intelligibility of the dialog [3]. The GEQ has become a standard tool in music studios, in public address systems for concerts, and in selected audio systems, such as in exclusive car radios and home stereo systems [4]. For a long time, the band filters of GEQs have been second-order analog bandpass filters, with their center frequencies locked at the control frequencies, such as the octaves or one-third octaves. Digital GEQs were developed since the late 1970s, mainly by converting analog designs to digital filters [5–8]. This naturally led to a set of digital biquad filters connected in parallel or in cascade [1]. This paper proposes a novel GEQ design based on cascading digital shelf filters.

Early digital GEQs had limited accuracy in approximating the magnitude response drawn by the target gains[1] [9,10], but major advances have been made in this millennium. In 2004, Abel and Berners showed that dB magnitude responses of digital second-order peak filters were highly self-similar when the gain was varied, but the center frequency was kept constant [11]. This allowed least-squares optimization of the filter gains, which led to accurate cascade GEQ designs using one second-order peak filter per band [10,12–14]. Also, accurate parallel GEQs may now be designed by first designing a cascade filter system and then converting it to the parallel form [15], which is advantageous for parallel computing [16]. Recent work showed that the number of active band filters can be minimized prior to designing the GEQ, thus offering the possibility to eliminate some filters, which leads to computational savings [17,18]. Furthermore, linear-phase GEQs have been proposed, also very recently, but they require the use of frequency-domain filtering [19,20] or high-order finite impulse response filters [21,22], causing more latency than biquad-filter-based GEQs and are not discussed further here.

This paper proposes to cascade first-, second-, or higher-order shelf filters at prescribed center frequencies to form the magnitude response of a GEQ. In practice, each shelving filter transitions the magnitude response from one center frequency to the next. Fig. 1 shows an illustrating example where a target magnitude response is approximated with a state-of-the-art conventional GEQ and with the proposed multi-shelf GEQ, which uses second-order shelving filters. The approximations have slight differences, mainly in the ripple of the magnitude response between the control points. Both designs lead to a minimum-phase system. Formerly, shelving filters have been used in audio mainly as bass and treble tone controls and for loudness compensation [1,4,23,24]. The low- and high-frequency shelving filters are also well suited to be used as the lowest and highest bands in a GEQ [1]. Abel and Berners [11] also proposed to use second-order shelving filters as building blocks of a cascade GEQ, but it remained to be shown whether this offered any advantage with respect to peak filters.

Some previous works have studied the use of shelving filters as building blocks for audio equalization. In 2006, Holters and Zölzer

* Corresponding author.
E-mail address: vesa.valimaki@aalto.fi (V. Välimäki).

[1] Target gains are occasionally called command gains in literature [1,2].

https://doi.org/10.1016/j.sigpro.2024.109630
Received 19 April 2024; Received in revised form 25 June 2024; Accepted 23 July 2024
Available online 26 July 2024

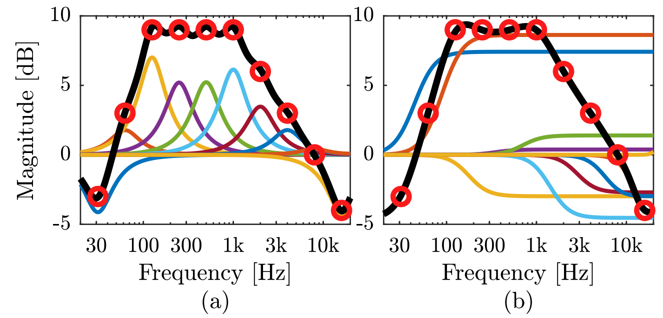

Fig. 1. Magnitude responses of GEQs based on (a) symmetric peaking biquad filters [13] and (b) the proposed second-order shelving filters. The colored lines show the individual band filters, the black line is the overall response, and the red circles are the target gains.

[25,26] introduced a closed-form design of shelving and band-shelving filters of arbitrary order, based on analog prototypes, and showed that they can be cascaded to implement a GEQ. Rämö and Välimäki studied the use of high-order Holters-Zölzer band-shelving filters in a GEQ. However, to obtain a 2-dB accuracy for a ±20-dB dynamic range the band filter orders became quite large, such as 20 or larger [27]. Fourth-order Holters-Zölzer band-shelf filters were also tested in a GEQ – without optimizing the filter gains – and were found to be less accurate than optimized second-order filters [9].

Jot [28] showed that a pair of second-order shelving filters could approximate a three-band equalizer. Also, a wideband approximation of a magnitude response with a constant slope, such as that corresponding to pink noise, could be accomplished [28]. Schultz et al. [29] used several second-order shelving filters to approximate various magnitude responses, such as a constant 3-dB slope. They showed that a cascade of shelving filters can be more suitable for this task than peak filters [29].

Our work takes the concept of shelf-filter-based GEQ further, describing a design method for a multi-shelf octave GEQ and comparing it with a state-of-the-art peak-filter-based GEQ. The results show that the proposed multi-shelf GEQ has a better dynamic range than what is possible to obtain with peak filters. Additionally, a better approximation accuracy can be obtained for many common settings using second-order shelf than peak filters, especially when the target response contains flat regions or smooth slopes doing up or down, namely because it is hard for the peak filters to form a flat response.

The rest of this paper is organized as follows. Section 2 reviews the design of cascade GEQs, the idea of self-similarity of filters, and recapitulates a state-of-the-art baseline design method. Section 3 introduces the proposed design. Section 4 compares the proposed method with the baseline and analyzes the results. Section 5 concludes this paper. The Matlab code to reproduce all figures is provided online.[2]

2. Background

This section describes the principles of cascaded GEQ design based on self-similar filters. The self-similarity turns the filter design into a least-squares optimization problem, which is suitable for real-time adjustments. The self-similarity also leads to simple designs of loop filters in recursive delay filters, which are proportional to the delay lengths [28,30,31].

[2] https://github.com/SebastianJiroSchlecht/MultiShelfGEQ.

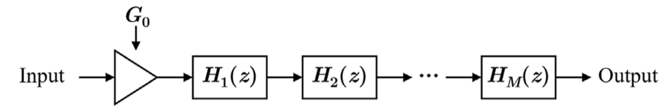

Fig. 2. Block diagram of cascade GEQ for M band filters. The multiplying coefficient G_0 represents the broadband gain.

2.1. Cascade GEQs

Given a target magnitude response $T(\omega_j)$ defined at a set of control frequencies $\omega_j \in [0,\pi]$ on the frequency axis, we want to determine a digital filter $H(z)$ closely following the magnitude response, i.e.,

$$\min_H \sum_j \left(\left|H(e^{\imath\omega_j})\right| - T(\omega_j)\right)^2, \tag{1}$$

where $\imath^2 = -1$. A cascade GEQ H comprises M band filters $H_i(z)$ in a serial connection, as shown in Fig. 2, and has the transfer function of the form

$$H(z) = G_0 \prod_{i=1}^{M} H_i(z). \tag{2}$$

where $G_0 \in \mathbb{R}_{\geqslant 0}$ is a broadband gain factor.

Solving (1) directly leads to a nonlinear problem. A common design trick is to convert the problem to the logarithmic scale [10–12], i.e.,

$$\min_H \sum_j \left(\log_{10}\left|H(e^{\imath\omega_j})\right| - \log_{10} T(\omega_j)\right)^2, \tag{3}$$

with

$$\log_{10}|H(z)| = \sum_{i=1}^{N} \log_{10}\left|H_i(z)\right|. \tag{4}$$

The design error in (3) is also minimized on the logarithmic scale, which leads to better auditory similarity [1]. We now choose a special class of low-order filters H_i, which are approximately self-similar, i.e.,

$$\log_{10}\left|H_i(e^{\imath\omega}; g_i)\right| \approx \frac{g_i}{p}\log_{10}\left|H_i(e^{\imath\omega}; p)\right|, \tag{5}$$

where $H(z;p)$ is a prototype filter with prototype gain p, as suggested by Oliver and Jot [10], and $g_i \in \mathbb{R}$ is the filter gain in decibel (dB).

The filter coefficients of $H(z;p)$ depend on the filter gain g. The accuracy of the self-similarity depends on the filter design, prototype gain, and filter gain. Usually, the self-similarity degrades the more different the prototype gain and the filter gain are. Therefore, the filter gain is limited between $\pm g_{\max}$. Using such self-similar filters, the GEQ design (3) can be cast to a constrained linear least-squares problem, i.e.,

$$\min_{g\in\mathbb{R}^{M\times 1}} \|\boldsymbol{H}\boldsymbol{g} - \boldsymbol{t}\|_2, \quad \text{s.t. } |g_i| \leqslant g_{\max} \quad \forall i = 1,\dots,M, \tag{6}$$

where $\|\cdot\|_2$ is the l2-norm and the matrix elements of $\boldsymbol{H}$ and $\boldsymbol{t}$ are

$$\begin{aligned} H_{ji} &= \frac{1}{p}\log_{10}\left|H_i(e^{\imath\omega_j}; p)\right| \\ t_j &= \log_{10} T(\omega_j). \end{aligned} \tag{7}$$

The matrix elements H_{ji} are the magnitude response of the ith prototype filter at the jth control frequency, and t_j is the target gain at that frequency. The vector $\boldsymbol{g} = [g_1,\dots,g_M]$ comprises the filter gains in (5). The optimization problem (6) can be efficiently solved, and the pseudo-inverse of the interaction matrix $\boldsymbol{H}$ can be pre-computed as it typically does not change during operation [12].

2.2. Self-similar filters

We review several self-similar low-order filters. The simplest is the broadband gain, i.e.,

$$H_{\text{broadband}}(z; g_0) = 10^{g_0/20} = G_0, \tag{8}$$

which is perfectly self-similar for any gain g_0. The broadband gain is used as the first stage in the cascaded GEQ; see Fig. 2.

The most common self-similar filter is the second-order peak-notch filter, often called a parametric equalizer [1,4,10], i.e.,

$$H_{\mathrm{PN}}(z) = \frac{\sqrt{G} + \alpha G - \left[2\sqrt{G}\cos(\omega_c)\right] z^{-1} + [\sqrt{G} - \alpha G] z^{-2}}{\sqrt{G} + \alpha - \left[2\sqrt{G}\cos(\omega_c)\right] z^{-1} + [\sqrt{G} - \alpha] z^{-2}}, \tag{9}$$

where $\alpha = \tan(B/2)$, B denotes the bandwidth, G is the (linear) filter gain, and ω_c defines the center frequency of the peak or notch in radians. There are several variations to the exact parametrization of this filter, leading to improved self-similarity at higher gains and extremal frequency bands. Typical bell-shaped magnitude responses and a comparison of normalized magnitude responses to reveal their similarity have been shown by Abel and Berners [11].

In this work, we propose to use self-similar shelving filters to cascade a GEQ. The first- and second-order shelving filters are popular equalizer designs [1]. A generalized form proposed by Holters and Zölzer [25] can be used to compute the first-, second-, and higher-order shelving filters. For the Kth-order low-shelving filter, the equation is given by

$$H_{\mathrm{LS},K}(z) = \prod_{k=1}^{K} \frac{R\gamma e^{\imath\alpha_k} + 1 + (R\gamma e^{\imath\alpha_k} - 1) z^{-1}}{R\frac{1}{\gamma} e^{\imath\alpha_k} + 1 + \left(R\frac{1}{\gamma} e^{\imath\alpha_k} - 1\right) z^{-1}}, \tag{10}$$

where $\gamma = \sqrt[2K]{G}$, $\alpha_k = \pi(0.5 - (2k-1)/2K)$, $R = \tan(\pi f_b / f_s)$, G is the linear filter gain, and f_b is called the break frequency, i.e., the frequency where the transfer function has half the gain $G/2$. The design is always stable since it is based on a stable s-domain formulation, and a subsequent bilinear transform preserves the stability [25]. The Kth-order high-shelf filter can be obtained by setting

$$H_{\mathrm{HS},K}(z) = H_{\mathrm{LS},K}(-z), \tag{11}$$

and by shifting the break frequency by $\pi(1 - 2f_b/f_s)$. The self-similarity of shelving filters is studied further in Section 3.

2.3. Baseline design: Symmetric graphic equalizer

As a baseline method against which the proposed method is compared, we have chosen the GEQ design by Liski et al. [13], representing the state-of-the-art among octave GEQ designs based on peak-notch filters. In this paper, we call this baseline the symmetric graphic equalizer, or SGE, because of the shape of its band filters [13]. As band filters, SGE uses peak-notch filters having approximately symmetric magnitude response across the whole frequency range [13]. This peak-notch filter design is based on an original method proposed by Orfanidis [32], which allows adjusting the filter gain not only at the center frequency but also at its band edges, at dc, and at the Nyquist limit, or at five distinct frequencies. In the baseline SGE method, the dc gain of all band filters is set to 1.0 [13]. However, at both band edges and at the Nyquist limit, the gain of each band filter is carefully adjusted based on the peak gain value to maintain self-similarity [13].

The transfer function of peak-notch filter used in SGE [13] can be written as

$$H_{\mathrm{S}}(z) = \frac{\frac{G_N + W^2 + A_2}{1 + W^2 + A_1} - 2\frac{G_N - W^2}{1 + W^2 + A_1} z^{-1} + \frac{G_N + W^2 - A_2}{1 + W^2 + A_1} z^{-2}}{1 - 2\frac{1 - W^2}{1 + W^2 + A_1} z^{-1} + \frac{1 + W^2 - A_1}{1 + W^2 + A_1} z^{-2}}, \tag{12}$$

where

$$W^2 = \sqrt{\frac{|G_m^2 - G_N^2|}{|G^2 - 1|}} \tan\left(\frac{\omega_c}{2}\right)^2,$$

$$A_1 = \sqrt{\frac{C + D}{|G^2 - G_B^2|}}, \quad A_2 = \sqrt{\frac{G^2 C + G_B^2 D}{|G^2 - G_B^2|}},$$

$$C = |G_B^2 - G_N^2| \Delta\Omega^2 - 2W^2\left(|G_B^2 - G_N| - \sqrt{|G_B^2 - 1||G_m^2 - G_N^2|}\right),$$

$$D = 2W^2\left(|G^2 - G_N| - \sqrt{|G^2 - 1||G^2 - G_N^2|}\right),$$

$$\Delta\Omega = \left(1 + \sqrt{\frac{|G_B^2 - 1|}{|G_B^2 - G_N^2|}} W^2\right)\alpha, \tag{13}$$

and G_B and G_N are the linear gains at the edges of the bandwidth B and at the Nyquist limit, respectively, and G_m is the linear gain of the mth filter. The bandwidth of the first six filters – those at the six lowest center frequencies – has been set to $B = 1.5\omega_c$ whereas the next four filters have their bandwidth adjusted smaller to obtain a symmetric behavior, and are 99.7%, 98.5%, 92.9%, and 43.3% of $1.5\omega_c$, respectively, when the sample rate is $f_s = 44.1$ kHz [13].

The baseline SGE design uses directly the dB target gains at the ten octave bands as input parameters and returns the optimized filter gains g_k in dB [13]. A prototype shape is selected for each band filter by using a prescribed prototype gain. To obtain a 1-dB accuracy for filter gains up to $g_{\max} = 12$ dB, the prototype dB-gains are 13.8, 14.5, 14.5, 14.6, 14.5, 14.5, 14.6, 14.6, 14.5, and 13.6 for the bands from the lowest to the highest octave [13]. The magnitude response samples of each prototype filter are divided by the prototype dB-gain to obtain basis functions with a peak gain of 1 dB. Another trick used in the SGE method to improve the design accuracy is to optimize the magnitude response not only at the octave center frequencies but also at their nine midpoints, which are obtained as geometric means of the adjacent octave centers [13]. The target magnitude at each intermediate point is the average of the neighboring target gains. A weighted least-squares design is used that has a weight 1.0 at the octave centers and a weight 0.5 at the nine midpoint frequencies [13].

After optimized peak dB-gains $\boldsymbol{g}$ are obtained, the SGE method sets the dB-gain at the bandwidth edges at $\boldsymbol{g}_B = 0.29\boldsymbol{g}$ for all band filters [13]. Liski et al. also optimized the Nyquist gain G_N of each band filter to obtain a symmetric bell-shaped magnitude response at the high end of the frequency range, and the actual value is obtained by evaluating a second-order polynomial of the peak dB-gain [13]. Finally, the band filter coefficients for the baseline SGE are obtained by converting the gain parameters from dB to the linear scale, $\boldsymbol{G}_m$, and using them in (12) and (13). The obtained peak-notch filters are cascaded as in Fig. 2.

3. Proposed method

This section first discusses the self-similarity of shelving filters and then how to combine them to form a multi-shelf GEQ. The sample rate f_s used in this study is 44.1 kHz.

3.1. Self-similarity of shelving filters

We study the self-similarity of the shelving filters as this is the crucial property to allow the log-domain least-squares design described by (6). To the best of our knowledge, this is the first thorough self-similarity evaluation of this filter type. We first show the self-similarity of the second-order shelving filter (10) with $K = 2$. Secondly, we show the self-similarity across different filter orders K.

For easier comparison of the shape of the magnitude response, we utilize the gain-normalized magnitude, i.e., $H(e^{\imath\omega_j}; g)/g$. Fig. 3 depicts the self-similarities of the first- and second-order shelving filters with gains g varying from 1 to 40 dB. Overall, the second-order filters with $K = 2$ are steeper than the first-order filters with $K = 1$. When the magnitudes are normalized, it can be observed that the shelving filters with lower gains have steeper slopes than those with higher gains. This contrasts the self-similarity of peak filters, which become steeper in the transition region for higher gains [1].

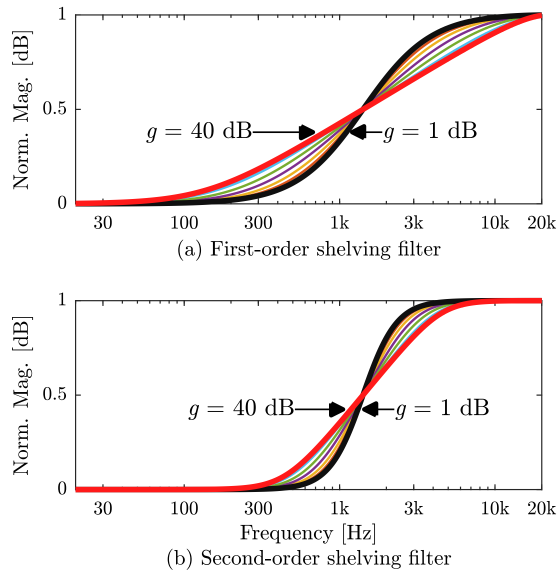

Fig. 3. Comparison of self-similarity of (a) first-order and (b) second-order high-shelf filters at different filter gains $g = [1, 6, 12, 18, 24, 30, 36, 40]$ dB, enabled by normalizing the filter dB magnitude responses by g. The break frequency is $f_b = 1414$ Hz.

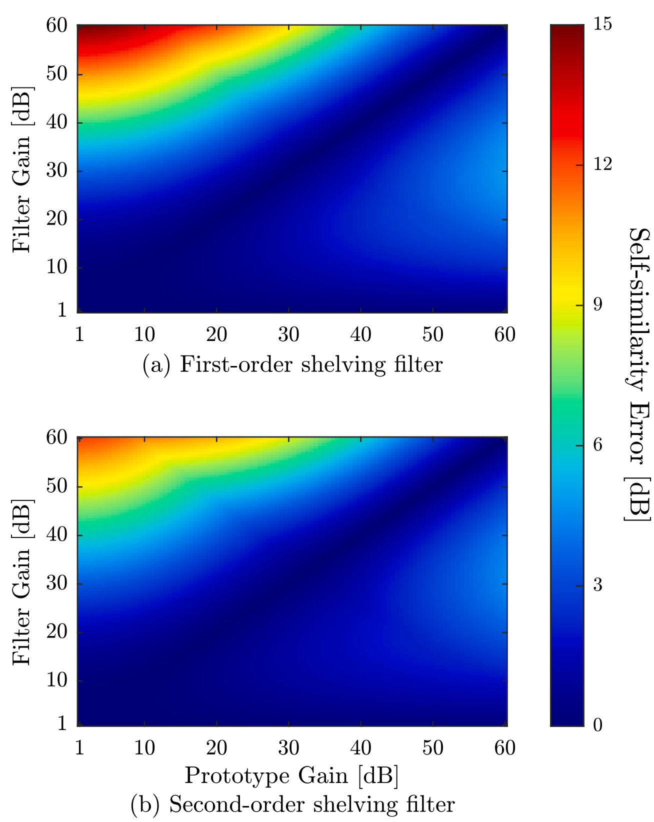

Fig. 4. Prototype gain p versus filter gain g self-similarity error (14) of (a) a first-order and (b) a second-order shelving filter, when $f_b = 1414$ Hz.

The self-similarity error can be quantified as the maximum deviation of the magnitude response at the control frequencies, i.e.,

$$\epsilon(g, p) = \max_j \left| \log_{10} \left| H(e^{\imath\omega_j}; g) \right| - \frac{g}{p} \log_{10} \left| H(e^{\imath\omega_j}; p) \right| \right| \tag{14}$$

Table 1
Octave center frequencies and their geometric midpoints, which are used as break frequencies of the shelving filters.

Octave frequency (Hz)	Midpoint frequency (Hz)
31.25	44.2
62.5	88.4
125	176.8
250	353.6
500	707.1
1000	1414
2000	2828
4000	5657
8000	11 314
16 000	N/A

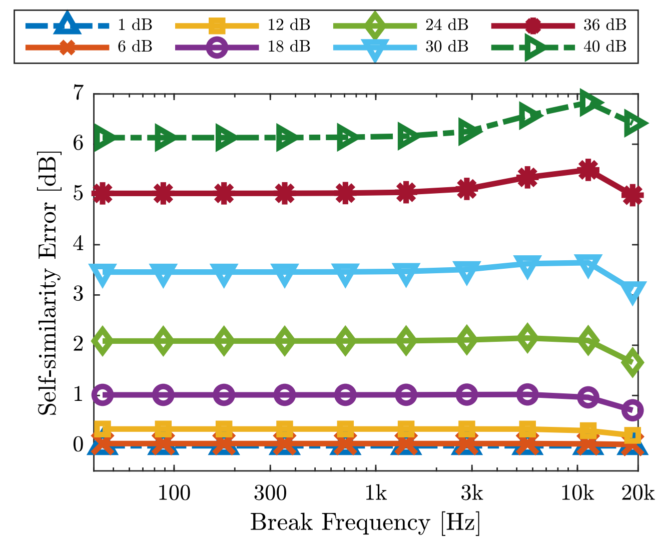

Fig. 5. Self-similarity error (14) of the second-order shelving filter with different break frequencies f_b and filter gains g, when the prototype gain p is 1 dB.

Fig. 4 depicts the maximum absolute errors for each prototype and filter gain combination. For equal prototype and filter gain, i.e., $g = p$, the error is always zero. The error increases with the difference between g and p. The self-similarity error alone suggests that the prototype gain should be close to the filter gain. Optimization schemes for peak filter GEQ previously used this argument to change the prototype gain iteratively [12,33].

For the shelving filter, as seen in Fig. 3, the higher prototype gains lead to shallower slopes, which limits the overall gain difference between frequency bands. We find that using a prototype gain of $p = 1$ dB is a good trade-off as the self-similarity error remains below ± 1 dB until the filter gain is approximately 18 dB.

We further show the band dependency of the self-similarity error. For this, we study the self-similarity of shelving filters with different break frequencies f_b. For an octave-band GEQ, we choose the break frequencies to be the geometric mean of the control frequencies. Both the octave center and the midpoint frequencies are listed in Table 1.

Fig. 5 shows the self-similarity errors for different break frequencies f_b of the second-order shelving filter (14) with prototype gain $p = 1$ dB. The error increases mostly independent of the filter band except for the two highest bands, which have a slightly higher self-similarity error. In peak-notch GEQs, the extremal bands require careful tuning; see Section 2.3. Similar techniques may be applied to the shelving filters. As the extra error is low, we leave this for further investigation.

From Figs. 3, 4, and 5, it is clear that the maximum filter gain g_{max} is limited by the self-similarity error, which in turn is due to the limited slope of the shelving filter at higher filter gains. In principle, the slope can be steepened without changing the filter order. However,

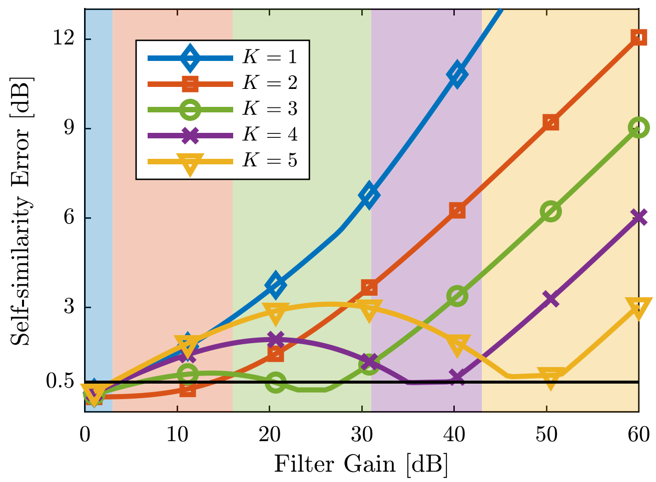

Fig. 6. Self-similarity error (15) across filter orders K for a shelving filter with f_b = 1414 Hz.

this comes at the cost of monotonicity of the magnitude response, which overshoots at the edges of the slope. Alternatively, we propose to dynamically switch the order of the shelving filter as higher-order filters generally have steeper slopes.

Based on the second-order filter, we quantify the self-similarity error for different orders K, i.e.,

$$\epsilon_K(g,p) = \max_j \left| \log_{10} \left| H_K(e^{\imath\omega_j};g) \right| - \frac{g}{p} \log_{10} \left| H_2(e^{\imath\omega_j};p) \right| \right|, \tag{15}$$

where $H_k(e^{\imath\omega_j};g)$ is the higher-order shelving filter as in (10). Fig. 6 shows the order-switching self-similarity error for $K = 1, 2, \ldots, 5$ and prototype gain $p = 1$ dB. The second-order curve (red) in Fig. 6 is identical to the 1-dB column in the surface plot in Fig. 4. The third-order curve (green) in Fig. 6 has a higher error for filter gains below 18 dB but is consistently lower for higher gains. Similarly, fourth- and fifth-order filters are dissimilar to the second-order filter at low filter gains, but there is a high-gain region for which the error is close to 1 dB. For the first-order filter (blue), the error is only low for gains below 3 dB but never lower than the second-order filter. A zeroth-order filter has trivially an error equal to the filter gain. While up-switching, i.e., increasing the filter order, can actually improve the self-similarity error, down-switching, i.e., decreasing the filter order, always increases the error. However, down-switching can lead instead to better computational efficiency.

From this, we can derive an order-switching scheme, where the filter order is changed to minimize the self-similarity error. Fig. 6 shows the colored regions where a given filter order gives the minimal error. Down-switching is only allowed if the error is not increased by more than 1 dB. Table 2 shows the boundary gains for the order switching.

In principle, the slope of higher-order filters can be reduced to match the second-order slope. By this, the error could be further reduced, and faster switching is encouraged. Depending on the application, self-similarity error can be traded against computational cost.

3.2. Proposed multi-shelf GEQ

We propose a GEQ based on shelving filters instead of the more common peak filters. The design procedure is the following:

- Set the control frequencies ω_j
- Set the break frequencies f_b of the shelving filters
- Set the prototype gain p and max gains $g_{\max}$
- Solve constrained linear least-squares problem (6) for a target magnitude response $T(\omega_j)$ to obtain filter gains $\boldsymbol{g}$
- (Optional) Select the shelving filter orders K_m for the mth filter
- Compute filter coefficients using (10).

Table 2
Variable order shelving filter switching criteria based on the filter gain g (dB).

		Shelving filter order					
		0	1	2	3	4	5
	1	⩽1	1–7	8–16	17–31	32–42	⩾43
	2	⩽1	1–7	8–16	17–31	32–42	⩾43
	3	⩽1	1–7	8–16	17–31	32–42	⩾43
	4	⩽1	1–7	8–16	17–31	32–42	⩾43
Octave band	5	⩽1	1–7	8–16	17–31	32–42	⩾43
	6	⩽1	1–7	8–16	17–31	32–42	⩾43
	7	⩽1	1–7	8–16	17–31	32–43	⩾44
	8	⩽1	1–7	8–16	17–31	32–43	⩾44
	9	⩽1	1–7	8–16	17–33	34–47	⩾48
	10	⩽1	1–7	8–16	17–36	37–52	⩾53

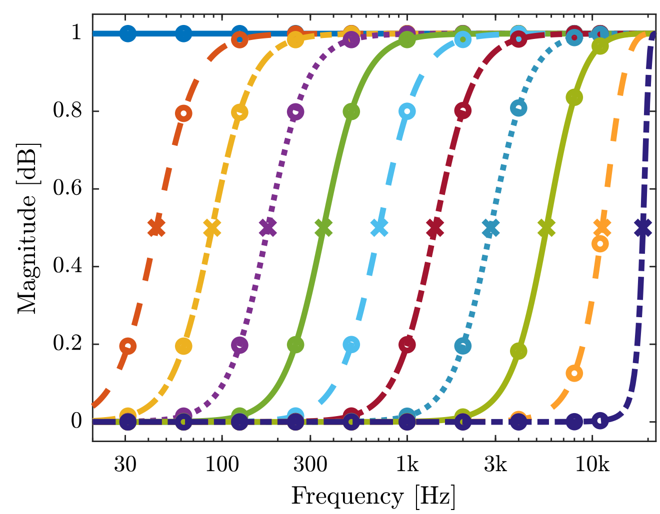

Fig. 7. Magnitude responses of the prototype second-order shelving filters and the broadband gain (solid blue line) used as basis functions in the least-squares optimization. The shelving filters have a fixed break frequency (marked by a cross) and a prototype gain of 1 dB. The circle markers indicate the frequency sampling points.

The design procedure offers several choices which can be customized for the application at hand. The control frequencies determine the resolution of the frequency axis as the least-squares approach (6) distributes error equally across all points. Alternatively, weighted least squares can be used to emphasize some control frequencies over others. More control frequencies lead to a tighter control of the response and a larger least-squares problem. Typical distribution of control frequencies follows an octave or one-third-octave spacing. In the following, as the control frequencies, we use the octave center frequencies shown in Table 1 and one frequency close to the Nyquist limit.

The set of break frequency f_b determines the number of shelving filters. The number of filters M in (2) is directly proportional to the processing cost. Also, the break frequency should generally follow the distribution of the control frequencies to allow fitting the target magnitude closely. For logarithmically spaced control frequencies, we have found that using the geometric means between those frequencies yields a good accuracy, see Table 1.

As discussed in Section 3, the prototype gain p impacts the self-similarity and the slope of the prototype filter. We have found that using a low prototype gain such as $p = 1$ dB yields a good compromise.

The maximum gain $g_{\max}$ constraints the least-squares solution and limits the impairment of the self-similarity. In general, the filter design has two types of errors: the least-squares fitting error $\boldsymbol{H}\boldsymbol{g} - \boldsymbol{t}$ in (6) and the self-similarity error (14). The fitting error can result from an overdetermined problem with more control frequencies than shelving

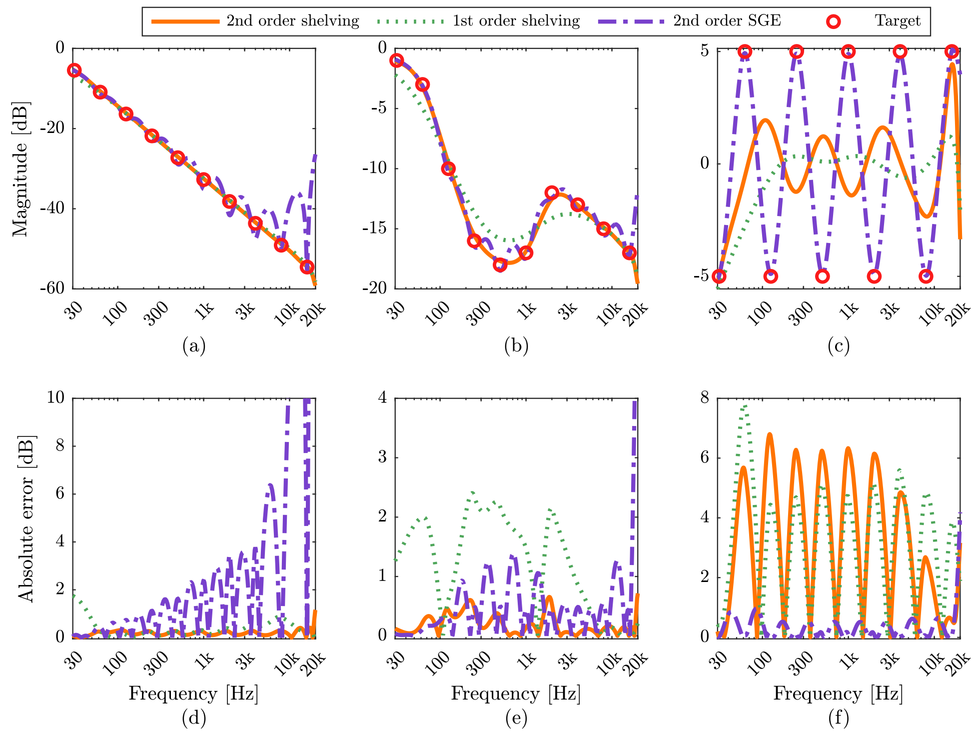

Fig. 8. Magnitude response and errors from three example cases for first- and second-order shelving GEQ and the baseline SGE method, which uses second-order peak filters.

filters. Further, the maximum gain constraint can lead to fitting error as the useable gain is limited. Thus, the maximum gain $g_{\max}$ gives a trade-off between the two error types where larger $g_{\max}$ reduces the fitting error but increases the self-similarity error. The matter is further complicated in particular cases as these two types of errors can cancel each other, yielding unexpectedly accurate results. We propose to design according to a target error tolerance of 1 dB. Thus, we choose the maximum gain $g_{\max}$ so the self-similarity error is below 1 dB. For a GEQ comprising only second-order sections, the $g_{\max} = 18$ dB, see Fig. 6. For an order-switching GEQ, the $g_{\max}$ is according to the 1-dB limit of the highest allowable order. For instance, with a maximum order of $K = 5$, the maximum gain $g_{\max}$ is 50 dB.

Fig. 7 shows the resulting ten prototype shelving filters and a broadband gain. The markers indicate the sampling of the prototype filters at the control frequencies, which form the interaction matrix $\boldsymbol{H}$ in (6). The filter gains $\boldsymbol{g}$ are computed by solving the problem in (6) and subsequently, we use to (10) to compute the filter coefficients.

4. Results

In the following, we present several design examples to evaluate the proposed multi-shelf GEQ. We compare three types of shelving GEQ comprising either first-order, second-order, or variable-order shelving filters. The control frequencies are chosen as octave frequency points and their midpoints; see Table 1. We use ten shelving filters at the break frequencies equal to the frequency midpoints. The maximum gain $g_{\max}$ is 10 dB for the first-order, 18 dB for the second-order, and 50 dB for the variable order. The variable-order design can dynamically choose $K = 0, 1, 2, 3, 4$, or 5 according to Table 2.

We compare our filter design against a state-of-the-art peak GEQ called SGE [13] also with ten second-order filters, which is described briefly in Section 2.3. The filter gains of SGE are determined similarly with a log-domain least squares [13]. The filter design error is given by the log-domain difference at the control frequencies, i.e.,

$$20|\log_{10}|H(e^{\imath\omega_j})| - \log_{10} T(\omega_j)|, \tag{16}$$

Fig. 8 demonstrates three target magnitude responses and several filter approximations.

The first case in Fig. 8(a) demonstrates the shelving GEQ capability to fit high-dynamic range targets. The target response decreases linearly from 0 to −60 dB. Both the first- and second-order shelving GEQ approximate the target closely. Fig. 8(d) shows the corresponding filter design error, which is below 3 dB for the first-order except at the lowest band and below 1.5 dB for the second-order GEQ. The SGE, in comparison, struggles with the large attenuation at the high frequencies. At such high target gains, the peak filters in the SGE become extremely pointy such that the response at the control frequencies is matched closely, but the errors in between reach more than 30 dB. This illustrates a major difference between the two GEQ designs. While the SGE attenuates each frequency band individually, the shelving GEQ attenuation is cumulative across frequency bands.

The second case in Fig. 8(b) is derived from a loop loss filter of a recursive artificial reverberator [34], which applies reverberation to a signal via delay, attenuation, and feedback operations. Frequency-dependent attenuation of a physical space often changes gradually across frequency. The shelving GEQs follow the target well: Fig. 8(b) shows errors below 2.1 dB for the first-order and below 0.3 dB for the second-order filters at the control frequencies. Also, the SGE performs with errors below 0.6 dB. However, the deviation between the control points is poor; for example, between 500 and 1000 Hz in Fig. 8(e), the error is almost 1.5 dB.

The third case in Fig. 8(c) demonstrates a limitation of the shelving GEQ as the target has a zig-zag shape, i.e., neighboring frequency bands have oscillating attenuation values. The first-order shelving filter fails and returns an almost completely flat response. The second-order shelving filter does not perform much better and yields a maximum error of almost 7 dB. In contrast, the SGE can match the zig-zag curve with an error below 1 dB. The zig-zag curve is unsuitable for the shelving GEQ as the filter slope is generally shallower than the peak filters.

Fig. 9 demonstrates three target magnitude responses for the variable order design. Two designs are considered using either up-only or up-down switching using Table 2. The resulting filter orders are

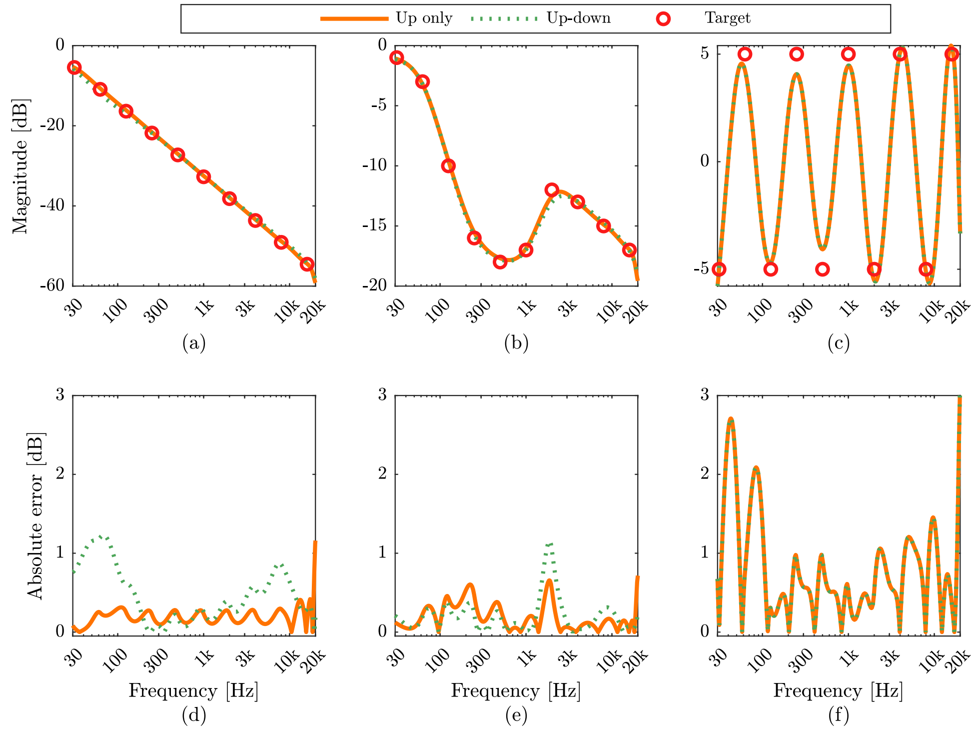

Fig. 9. Magnitude response and errors from three example cases for variable-order shelving GEQ. The filter orders of the ten shelving filters using up-down switching are (a) $K_m = [1, 1, 1, 1, 1, 1, 1, 1, 1, 1]$, (b) $K_m = [1, 2, 2, 1, 1, 2, 1, 1, 1, 1]$, and (c) $K_m = [3, 4, 4, 4, 4, 4, 4, 3, 3, 2]$. For the up-only switching, only orders $K_m \geqslant 2$ are used.

indicated in the figure caption. For the high-dynamic range target Fig. 9(a), only the lowest band can potentially be down-switched, leading to slightly lower computational cost. For the artificial reverb target Fig. 9(b), all bands can be down-switched such that the cumulative filter order is 10 instead of 20, i.e., a 50% reduction is achieved. The error, as indicated in Fig. 9(e), remains largely similar except at the Nyquist limit. The zig-zag target in Fig. 9(c) is more closely matched with the up-switching scheme at the cost of higher overall computational cost. The cumulative filter order is 35, which is an increase of 75% over the SGE design. Overall, one can observe that the multi-shelf GEQ exhibits less ripple between the control points than the SGE (cf. Fig. 8) by smoothly interpolating the target response.

5. Conclusion

In this paper, we propose the shelving GEQ as an alternative filter design method. The proposed method uses the log-scale least-squares optimization based on the self-similarity of the shelving filter. The shelving filter's slope limits the range of the self-similarity, such that the useable gain ranges from 0 to 18 dB for a second-order filter. In three target response examples, we demonstrated that the shelving GEQ accurately approximates smoothly varying target responses even with a high dynamic range. On the contrary, the shelving GEQ performs poorly with rapidly varying responses, whereas the state-of-the-art SGE remains superior in such cases.

For larger gain ranges, we proposed the variable-order shelving GEQ, where the shelving-filter order is up or down-switched dynamically based on the filter gain. The down-switching offers computational savings for responses that are well-approximated by shallower filters, and the up-switching allows fitting steeper responses without changing the overall filter design. The least-squares optimization can be updated with little computation, so the method is well suited for real-time audio applications.

To the best of our knowledge, the present paper is the first to propose a GEQ design based on shelving filters such that many fine-tunings known for other GEQ designs can be adapted in the future. The self-similarity of the shelving filter can be further improved, which directly leads to higher filter design accuracy. For instance, the shelving slope may be adjusted according to the filter gain. It is also conceivable to dynamically combine shelving and peak-notch filters in the optimization scheme for maximum flexibility.

CRediT authorship contribution statement

Sebastian J. Schlecht: Writing – review & editing, Writing – original draft, Visualization, Validation, Supervision, Software, Project administration, Methodology, Investigation, Formal analysis, Data curation, Conceptualization. **Tantep Sinjanakhom:** Writing – review & editing, Visualization, Validation, Software, Data curation. **Vesa Välimäki:** Writing – review & editing, Visualization, Supervision, Project administration, Investigation.

Declaration of competing interest

The authors declare that they have no known competing financial interests or personal relationships that could have appeared to influence the work reported in this paper.

Data availability

https://github.com/SebastianJiroSchlecht/MultiShelfGEQ.

References

[1] V. Välimäki, J.D. Reiss, All about audio equalization: Solutions and frontiers, Appl. Sci. 6 (129/5) (2016) 1–46, http://dx.doi.org/10.3390/app6050129.
[2] S. Nercessian, Neural parametric equalizer matching using differentiable biquads, in: Proc. Int. Conf. Digital Audio Effects, DAFx, online, 2020, pp. 265–272.
[3] D.A. Bohn, Operator adjustable equalizers: An overview, in: Proc. Audio Eng. Soc. 6th Int. Conf. Sound Reinforcement, Nashville, TN, 1988, pp. 369–381.
[4] J.D. Reiss, A.P. McPherson, Audio Effects: Theory, Implementation and Application, CRC Press, Boca Raton, FL, 2015.

[5] Y. Hirata, Digitalization of conventional analog filters for recording use, J. Audio Eng. Soc. 29 (5) (1981) 333–337.
[6] S.A. White, Design of a digital biquadratic peaking or notch filter for digital audio equalization, J. Audio Eng. Soc. 34 (6) (1986) 479–483.
[7] P.A. Regalia, S.K. Mitra, Tunable digital frequency response equalization filters, IEEE Trans. Acoust. Speech Signal Process. 35 (1) (1987) 118–120.
[8] C.C. Darabundit, J.S. Abel, D. Berners, Nyquist band transform: An order-preserving transform for bandlimited discretization, J. Audio Eng. Soc. 70 (9) (2022) 674–689.
[9] J. Rämö, V. Välimäki, B. Bank, High-precision parallel graphic equalizer, IEEE/ACM Trans. Audio Speech Lang. Process. 22 (12) (2014) 1894–1904.
[10] R.J. Oliver, J.-M. Jot, Efficient multi-band digital audio graphic equalizer with accurate frequency response control, in: Proc. Audio Eng. Soc. 139th Conv., New York, NY, 2015.
[11] J.S. Abel, D.P. Berners, Filter design using second-order peaking and shelving sections, in: Proc. Int. Comput. Music Conf., Miami, FL, USA, 2004, pp. 1–4.
[12] V. Välimäki, J. Liski, Accurate cascade graphic equalizer, IEEE Signal Process. Lett. 24 (2) (2017) 176–180, http://dx.doi.org/10.1109/lsp.2016.2645280.
[13] J. Liski, J. Rämö, V. Välimäki, Graphic equalizer design with symmetric biquad filters, in: Proc. IEEE Workshop Appl. Signal Process. Audio Acoust., WASPAA, New Paltz, NY, 2019, pp. 55–59.
[14] V. Välimäki, J. Rämö, Neurally controlled graphic equalizer, IEEE/ACM Trans. Audio Speech Lang. Process. 27 (12) (2019) 2140–2149, http://dx.doi.org/10.1109/TASLP.2019.2935809.
[15] J. Liski, B. Bank, J.O. Smith, V. Välimäki, Converting series biquad filters into delayed parallel form: Application to graphic equalizers, IEEE Trans. Signal Process. 67 (14) (2019) 3785–3795, http://dx.doi.org/10.1109/TSP.2019.2919419.
[16] J.A. Belloch, J. Badía, G. León, B. Bank, V. Välimäki, Multicore implementation of a multichannel parallel graphic equalizer, J. Supercomput. 78 (2022) 15715–15729, http://dx.doi.org/10.1007/s11227-022-04495-3.
[17] Y. Li, J. Yang, Q. Feng, W.-K.B. Ling, A design method for low-order accurate parallel graphic equalizers, J. Audio Eng. Soc. 70 (4) (2022) 284–293.
[18] M. Antonelli, J. Liski, V. Välimäki, Sparse graphic equalizer design, IEEE Signal Process. Lett. 29 (2022) 1659–1663, http://dx.doi.org/10.1109/LSP.2022.3191267.
[19] H. Schöpp, H. Hetze, A linear-phase 512-band graphic equalizer using the fast-Fourier transform, in: Proc. 96th Conv. Audio Eng. Soc., Amsterdam, The Netherlands, 1994, paper 3816.
[20] S. Cecchi, L. Palestini, E. Moretti, F. Piazza, A new approach to digital audio equalization, in: Proc. IEEE Workshop Appl. Signal Process. Audio Acoust., WASPAA, New Paltz, NY, 2007, pp. 62–65.
[21] D.S. McGrath, An efficient 30-band graphic equalizer implementation for a low-cost DSP processor, in: Proc. 95th Conv. Audio Eng. Soc., New York, NY, 1993, paper 3756.
[22] V. Bruschi, V. Välimäki, J. Liski, S. Cecchi, Linear-phase octave graphic equalizer, J. Audio Eng. Soc. 70 (6) (2022) 435–445, http://dx.doi.org/10.17743/jaes.2022.0014.
[23] T. Holman, F. Kampmann, Loudness compensation: Use and abuse, J. Audio Eng. Soc. 26 (7/8) (1978) 526–536.
[24] L. Fierro, J. Rämö, V. Välimäki, Adaptive loudness compensation in music listening, in: Proc. Sound Music Computing Conf., Malaga, Spain, 2019, pp. 135–142.
[25] M. Holters, U. Zölzer, Parametric higher-order shelving filters, in: European Signal Process. Conf., EUSIPCO, Florence, Italy, 2006, pp. 1–4.
[26] M. Holters, U. Zölzer, Graphic equalizer design using higher-order recursive filters, in: Proc. Int. Conf. Digital Audio Effects, DAFx, Montreal, Canada, 2006, pp. 37–40.
[27] J. Rämö, V. Välimäki, Optimizing a high-order graphic equalizer for audio processing, IEEE Signal Process. Lett. 21 (3) (2014) 301–305.
[28] J.M. Jot, Proportional parametric equalizers—Application to digital reverberation and environmental audio processing, in: Proc. Audio Eng. Soc. 139th Conv., New York, NY, 2015, pp. 1–8, URL http://www.aes.org/e-lib/browse.cfm?elib=17916.
[29] F. Schultz, N. Hahn, S. Spors, Shelving filter cascade with adjustable transition slope and bandwidth, in: Proc. Audio Eng. Soc. 148th Conv., online, 2020.
[30] J.M. Jot, A. Chaigne, Digital delay networks for designing artificial reverberators, in: Proc. Audio Eng. Soc. 90th Conv., Paris, France, 1991, pp. 1–12.
[31] K. Prawda, S.J. Schlecht, V. Välimäki, Improved reverberation time control for feedback delay networks, in: Proc. 22nd Int. Conf. Digital Audio Effects, DAFx, Birmingham, UK, 2019, pp. 299–306.
[32] S.J. Orfanidis, Introduction to Signal Processing, Prentice-Hall, Upper Saddle River, NJ, 1996.
[33] J. Liski, V. Välimäki, The quest for the best graphic equalizer, in: Proc. Int. Conf. Digital Audio Effects, DAFx-17, Edinburgh, UK, 2017, pp. 95–102.
[34] V. Välimäki, K. Prawda, S.J. Schlecht, Two-stage attenuation filter for artificial reverberation, IEEE Signal Process. Lett. 31 (2024) 391–395, http://dx.doi.org/10.1109/lsp.2024.3352510.